

## CREATION AND TEST OF MCNP NEUTRON LIBRARIES FOR NEUTRON CAPTURE ON GERMANIUM

**F. LOCHE and F. JALLU**

French Atomic Energy Commission  
CEA/DEN/CAD DTN/SMTM/LMN Build 225  
F-13108 SAINT PAUL LEZ DURANCE CEDEX  
florence.loche@cea.fr; fanny.jallu@cea.fr

### ABSTRACT

In the field of active gamma-ray spectrometry studies, including the neutron activation analysis, neutron scattering ( $n, n'\gamma$ ) and neutron capture ( $n, \gamma$ ) interactions, gamma-ray spectra resulting from neutron irradiation are measured using a HPGe detector.

Preliminary comparisons between experimental and MCNP [1] calculated spectra achieved good results, but no Ge gamma-ray appears in the calculated signal. In order to take into account the physical phenomena occurring within the detector itself, it is necessary to create a MCNP-compatible data table containing the discrete ( $n, \gamma$ ) gamma-rays produced in germanium.

Nuclear data, i.e. gamma-ray energies and intensities, published in the literature have been compared, leading to the choice of J.K. Tuli's data [2] to build "12-102" and "14-102" sections compatible with ENDF data format files for each of the five natural germanium isotopes. The completed files are compiled using the NJOY nuclear data processing code in order to create the MCNP-compatible files.

This paper presents the purpose of this work, as well as some preliminary comparisons between experimental and calculated results. The germanium data files created for the MCNP calculation and the results of the tests carried out in order to check the quality of these files are also provided.

*Key Words:* gamma-ray spectrometry, neutron capture, germanium, nuclear data

### 1 INTRODUCTION

The characterization of nuclear and non-nuclear materials requires qualified measurement methods as well as accurate nuclear data. Many methods have been developed and used in either industrial or research fields: passive gamma-ray spectrometry, self-induced X-ray fluorescence spectrometry [3], passive and active neutron measurement methods [4], radiography and tomography [5], induced photofission interrogation, active gamma-ray spectrometry [6]...

Active gamma-ray spectrometry uses the potentialities of neutron interactions to identify and quantify the isotopic or global components of a given object. Neutron reactions under interest are:

- activation reactions ( $n, 2n$ ), ( $n, p$ ), ( $n, \alpha$ ) leading to radioactive nuclides identified by their lifetime and the emitted gamma-ray energy,
- neutron scattering ( $n, n'\gamma$ ) and neutron capture ( $n, \gamma$ ) reactions occurring on nuclides that can therefore be recognized using the emitted gamma-ray energy and intensity.

For all these techniques, the knowledge and use of accurate nuclear data are of essential interest for a better understanding of physical phenomena and for accurate analysis results. Furthermore, the use of calculation codes in pre- and post-experimental development phases requires even more precise data, otherwise great errors may appear.

This paper deals with active gamma-ray spectrometry applied to the characterization of radioactive waste drum matrices. The interests of the neutron capture reactions are investigated in order to identify and quantify the components of neutron influence, i.e. moderation and absorption properties. Gamma-ray spectra are often measured using a gamma-ray detector containing germanium (High Purity Germanium – HPGe - semi-conductor).

In this application, the Monte Carlo N-Particle transport code MCNP [1] is used in two ways: modelling and dimensioning assay systems, and completing and helping signal analysis. The reliability of MCNP results depends on the accuracy of the nuclear data libraries adopted by the user. The last library distributed with MCNP4C2 is ENDF/B-VI-release 1 (Evaluated Nuclear Data File, version B-6, release 1) [7, 8]. It contains neutron capture data for most of the natural or isotopic elements of interest, but no Ge gamma-rays are available.

The purpose of the work presented in this paper is then to build, test and validate a new Ge data file compatible with MCNP.

## 2 PRELIMINARY CALCULATION STUDIES

### 2.1 Description of the Calculation Methodology

Gamma-ray spectra resulting from neutron irradiation are measured using a HPGe detector surrounded by a boron carbide (B<sub>4</sub>C) thermal neutron protection. A <sup>60</sup>Co isotopic source is placed in the very front of the detector in order to monitor the electronic dead-time. The whole setup mainly contains graphite and aluminum.

Following the experimental phase, MCNP4C2 calculations are done in order to help in analyzing measurement results. The geometry part of the MCNP4C2 entry file takes into account all details of the experimental setup, including for instance the concrete assay room walls, roof and ground.

As gamma-ray spectra cannot be directly calculated in a neutron-photon mode, two calculation steps are necessary. Firstly, a F5 tally collects the gamma-rays produced at a point placed in front of the detector (neutron-photon mode). Then, the F5 gamma-ray spectrum is described as a surface source placed in front of the detector, and gamma-rays are detected in the volume of the detector with a F8 tally (photon mode). The contribution of the <sup>60</sup>Co source, directly calculated as a F8 tally, is added to the previous final result.

Calculations are made using the MCNP4C2 code, and the ENDF/B-VI release 1 (.60c) neutron data libraries. Only few materials of the setup description require former data libraries (rmccs or endl92 [9]).

## 2.2 Preliminary Results

Calculated results are normalized in order to take into account the pulsed neutron source intensity ( $\approx 10^8 \text{ s}^{-1} [4\pi]$ ) and the measurement time. Fig. 1 shows the comparison of an experimental signal (pink) and the corresponding calculated spectrum (blue).

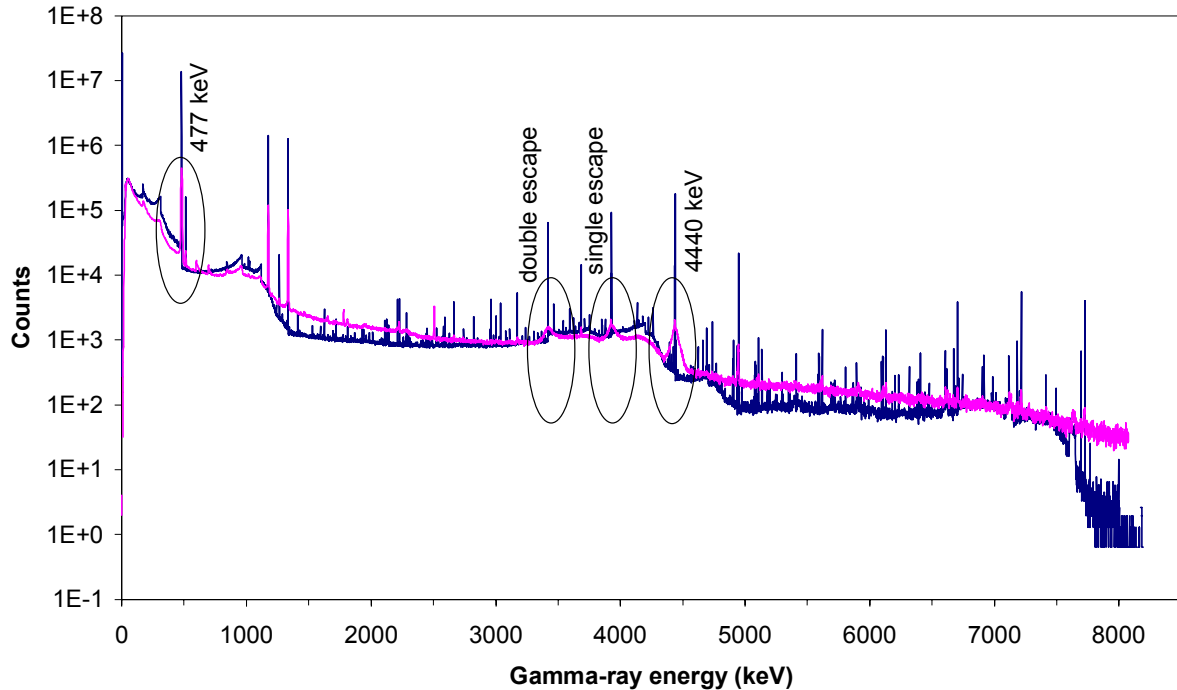


**Figure 1. Comparison of an experimental (pink) and a calculated (blue) spectra.**

The comparison between experimental and calculated spectra leads to good results: average level of the spectra is well adjusted and most of the experimental gamma-rays find their equivalent on the calculated spectra. The differences between the two signals mainly come from missing gamma-rays in the nuclear data tables (§ 2.3), and from the coincident counting rate and pulse pile-up due to electronics that can not be taken into account by MCNP.

Furthermore, the use of boron carbide around the HPGe detector leads to the appearance of a widened 477 keV peak resulting from the Doppler effect in the  $^{10}\text{B}(n,\alpha)^7\text{Li}^*$  reaction. Besides, carbon contained in graphite and boron carbide leads to the  $\text{C}(n,n'\gamma)$  4440 keV gamma-ray, whose broadening due to inelastic neutron scattering is not described in MCNP. Moreover, some gamma-rays are missing in the ENDF/B-VI release 1 data library: Fe  $(n,\gamma)$  discrete gamma-rays are described as 50 keV bins (Fig. 2) [10], and no Ge gamma-rays are available (Fig. 3).

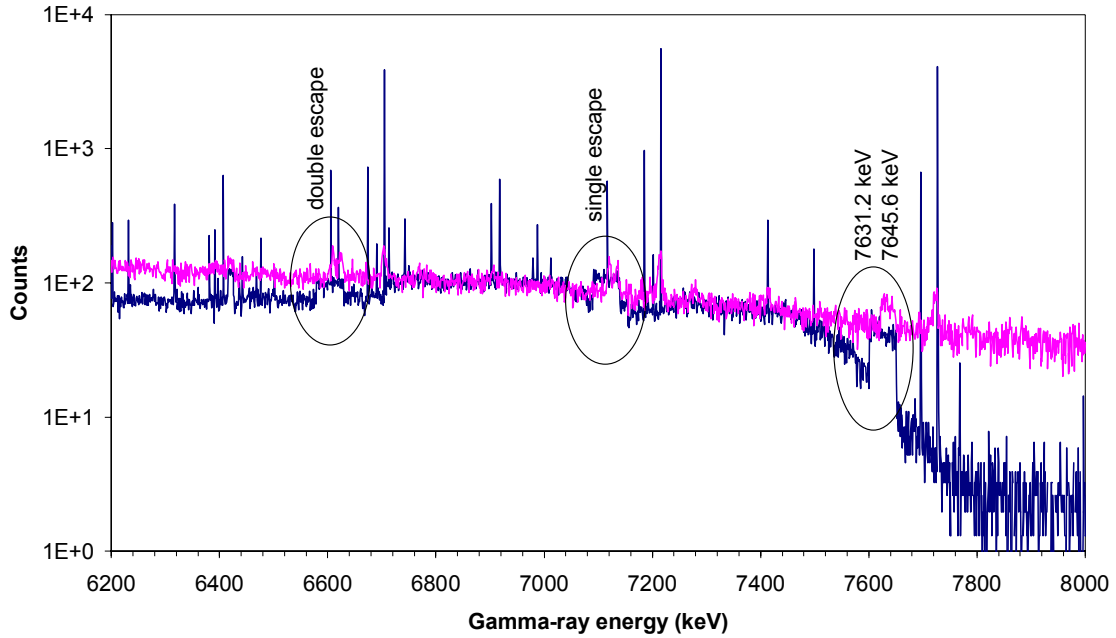


Figure 2. The Fe gamma-rays of 7645.6 keV and 7631.2 keV energies are described as a 50 keV bin in the ENDF/B-VI release 1 nuclear data library (blue).

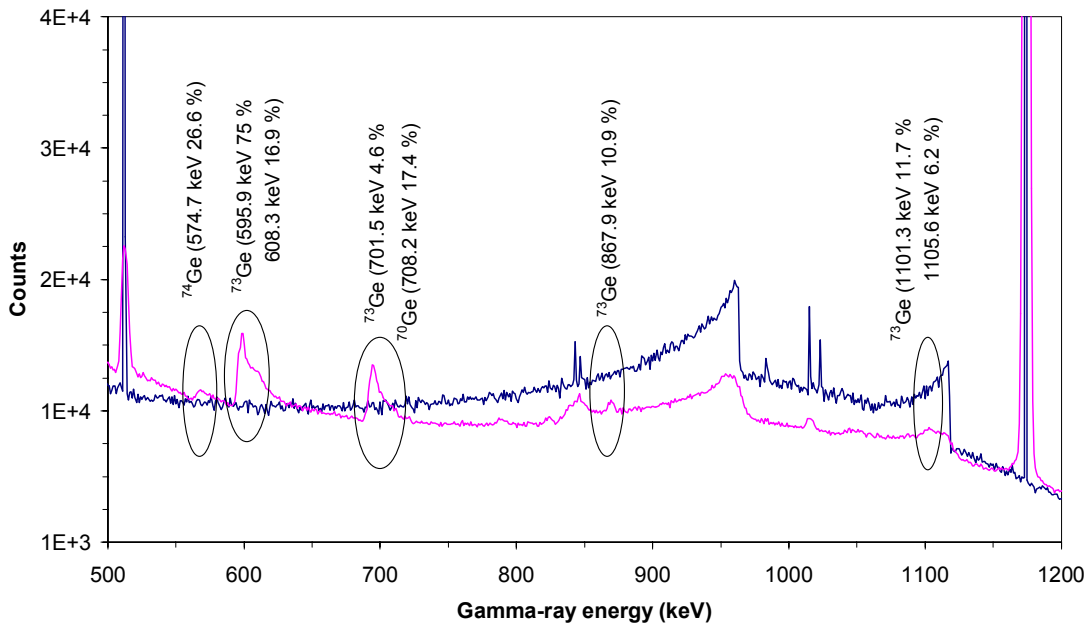


Figure 3. Absence of the Ge gamma-rays in the nuclear data libraries used by MCNP4C2.

### 2.3 Data Comparison

As shown above, further calculations require more accurate nuclear data, in particular concerning germanium. Preliminary to any data table creation, a detailed study of the ENDF data must be conducted for the main components of interest in the experimental setup. This can be done by means of the DISCEGAM (DIScrete-ENERgy GAMma-rays) files [11]. The data presented in these files are extracted from the original ENDF/B data libraries. Gamma-rays energy and intensity as well as cross-section reactions given for three incident neutron energies (thermal, 1 MeV and 14 MeV) are available, leading to a first analysis of the following ENDF data libraries: ENDF/B-V and ENDF/B-VI release 1, release 6 [12], and release 8 [13].

Referring to the DISCEGAM files, Table I compares the  $(n,\gamma)$ ,  $(n,n'\gamma)$ ,  $(n,x)$  discrete gamma-rays contained in the ENDF/B-VI release 1 and ENDF/B-VI release 8 libraries. The mention 'no data' means that no information is given for this element in the corresponding DISCEGAM file. The mention 'no data added' means that no new data appears in ENDF/B-VI release 8 compared to the former release.

**Table I. Comparison of  $(n,\gamma)$ ,  $(n,n'\gamma)$  and  $(n,x)$  data between ENDF/B-VI release 1 and release 8 libraries for the main components of the experimental setup description.**

Element	ENDF/B-VI release 1 [7]	ENDF/B-VI release 8 [13]
H	One $(n,\gamma)$ gamma-ray, the same.	
B	Isotopic data ( $^{10}\text{B}$ , $^{11}\text{B}$ ); $(n,\gamma)$ , $(n,n'\gamma)$ , $(n,p)$ , $(n,\alpha)$ , $(n,n'\alpha)$ gamma-rays.	No data added.
C	$(n,\gamma)$ , $(n,n'\gamma)$ gamma-rays.	No data added.
O	$(n,\gamma)$ , $(n,n'\gamma)$ , $(n,p)$ , $(n,\alpha)$ , $(n,n'\alpha)$ gamma-rays.	$(n,d)$ , $(n,t)$ , $(n,n'\alpha)$ and $(n,2n)$ gamma-rays are added.
Al	$(n,\gamma)$ , $(n,n'\gamma)$ , $(n,p)$ , $(n,n'p)$ gamma-rays.	$(n,\gamma)$ $(n,n'\gamma)$ , $(n,p)$ , $(n,\alpha)$ , $(n,t)$ , $(n,d)$ gamma-rays are added.
Si	$(n,\gamma)$ , $(n,n'\gamma)$ gamma-rays.	Isotopic ( $^{28}\text{Si}$ , $^{29}\text{Si}$ , $^{30}\text{Si}$ ) ; $(n,\gamma)$ , $(n,n'\gamma)$ , $(n,p)$ , $(n,\alpha)$ gamma-rays are added..
Fe	Isotopic data ( $^{54}\text{Fe}$ , $^{56}\text{Fe}$ , $^{57}\text{Fe}$ , $^{58}\text{Fe}$ ) ; $(n,n'\gamma)$ gamma-rays.	Isotopic data ; $(n,\gamma)$ gamma-rays are added.
Ge	No data.	

Table I clearly shows that ENDF/B-VI release 8 library is updated. For many elements, new discrete gamma-rays are added to the former release. For example, Fe  $(n,\gamma)$  gamma-rays are now described as discrete gamma-rays. However, no Ge discrete gamma-rays are yet available. Existing Ge data files found in release 8 [13,14] only contain  $(n,\gamma)$  cross sections, and the creation of complete tables became then essential to our work.

### 3 CREATION OF GE DATA TABLES

After identifying the existing Ge data files, they are completed on the base of  $(n,\gamma)$  data published in the literature, and different tests are conducted in order to validate the created files.

#### 3.1 Description of the Existing Ge Data Files

The DISCEGAM data are extracted from ENDF files. These ENDF files require a compilation to be read by the MCNP code. This compilation creates xsdir lines and a data file in ACE format [15]. ENDF data files are not directly usable by the MCNP code, and must be compiled in ACE format before use. As this kind of format is very complex and cannot be hand-written, we chose to create original files in ENDF format based on existing ones and documented in [8].

ENDF files already exist for the five natural isotopes of Ge ( $^{70}\text{Ge}$ ,  $^{72}\text{Ge}$ ,  $^{73}\text{Ge}$ ,  $^{74}\text{Ge}$  and  $^{76}\text{Ge}$ ) in the JEFF3.0 data library [16], and only for four of them in the ENDF/B-VI release 8 library. The existing JEFF3.0 files were then completed using the ENDF file format.

According to [8], the data contained in the ENDF format are classified in files and sections, a section being a subdivision of a file. Each file is identified by a parameter called MF, while each section is relative to MT. Each file contains specific data: for example, MF = 3 contains reaction cross sections, MF = 12 contains multiplicities for photon production (energies and intensities of the gamma-rays)... A section contains specific reaction information: for example, MT = 102 is relative to neutron capture. A section will then be named using the parameter MF-MT.

Concerning photon production data, the 3-102 section (gamma production cross section data) only composed the existing Ge data files. The 12-102 section (discrete gamma-ray energy and intensity data) and the 14-102 one (angular distribution of the gamma-ray emission) are the sections to be created.

#### 3.2 Bibliographical Data Research

Based on the four following published information sources containing discrete gamma ray energy and intensity data found in the literature, data were compared and chosen:

1. Lone's data: discrete gamma-rays energies and intensities for  $^{\text{nat}}\text{Ge}$  [17];
2. J.K. Tuli's database: isotopic discrete gamma-rays energies and relative intensities (normalized to the upper intensity) [2];
3. Updated data published in [18] includes isotopic Ge discrete gamma-rays energies and intensities.
4. The experimental EXFOR database [19], gives three references [20-22] containing discrete gamma-rays energies and intensities for some of the five Ge isotopes;

Table II presents the data comparison between the four previous references for the  $^{76}\text{Ge}$  isotope. Similar comparisons have been made for the four other isotopes, leading to the following conclusion: the most complete reference seems to be J.K. Tuli's database but it uses relative intensities whereas MCNP requires absolute intensities. The relative intensities are corrected using most frequently LANL data.

**Table II. Comparison of the  $^{76}\text{Ge}$  (n, $\gamma$ ) energies and intensities found in the literature and determination of absolute intensities (A.I.) from relatives ones (R.I.) extracted from [2]**

J.K. Tuli [2]			S.C. Frankle and al. [18]		EXFOR [20]	
$E_\gamma$ (keV)	R.I. $I_\gamma / I_{\gamma\text{max}}$ (%)	A.I. $I_\gamma$ (%)	$E_\gamma$ (keV)	A.I. $I_\gamma$ (%)	$E_\gamma$ (keV)	R.I. $I_\gamma / I_{\gamma 596 \text{ keV}}$ (%)
159.50	6.88	0.64	159.50	0.64	159.30	0.18
195.60	3.23	0.30	195.60	0.3		
431.50	17.63	1.63	431.50	1.64		
808.20	48.39	4.48	808.20	4.5		
850.80	34.84	3.23	850.80	3.24		
3895.20	23.23	2.15	3895.20	2.144		
4008.50	16.13	1.49	4008.50	1.488		
4193.20	53.76	4.98	4193.20	4.944		
4514.30	5.16	0.48	4514.30	0.48		
4821.80	3.44	0.32	4821.80	0.32		
5049.10	58.06	5.38	5049.10	5.386		
5420.10	16.13	1.49	5420.10	1.488		
5444.70	5.38	0.50	5444.70	0.496		
5912.85	100	9.27	5912.90	9.266		

### 3.3 Ge Data File Creation

Using J.K. Tuli's database, and according to the ENDF file format, sections 12-102 and 14-102 are created for each of the five Ge isotopes. Fig. 4 presents the structure of a MF = 12 file.

HEAD, TAB1, TAB2 and SEND (Section END) appear only for the user's comprehension. The sequence "MAT 12 102 N<sup>o</sup>" appears at the end of each line except the last one. MAT defines the isotope, N<sup>o</sup> is the section line number.

The HEAD line contains general information: ZA (Z\*1000+A) identifies the isotope, AWR is the ratio of the isotope mass to the neutron one, LO = 1 indicates that gamma-ray intensities are described, NK is the number of described gamma-rays. The zeros added in the line just complete this line but have no physical meaning.

The three TAB1 lines check the data using the sum of the intensity (Y(E)) for each incident neutron energy.

Each TAB2 contains NP pairs of data relative to one discrete gamma-ray energy (EG<sub>k</sub> given in eV): each pair of data is composed of one neutron energy (E given in eV) and the corresponding gamma-ray intensity (y<sub>k</sub>(E)). The NK gamma-ray energies are presented in decreasing order.

```

HEAD :      ZA      AWR  LO   0   NK   0  MAT 12 MT   1
TAB1 : 0.000000+0 0.000000+0   0   0   NR   NP  MAT 12 MT   2
      Eint: (NBT, INT)                                MAT 12 MT   N°
      Y (E) : (E, Y)                                MAT 12 MT   N°
TAB2 :      EG(k=1)      ES(k=1)  LP   LF   NR   NP  MAT 12 MT   N°
      Eint: (NBT, INT)                                MAT 12 MT   N°
      Yk (E) : (E, Yk)                            MAT 12 MT   N°
      ... k = 2...
      ... k = 3...
      .....
      ... k = NK...
SEND : 0.000000+0 0.000000+0   0   0   0   0  MAT 12 099999
    
```

Figure 4. Structure of a MF = 12 file.

The 3-102 sections already existing in the ENDF/B-VI release 8 and JEFF3.0 libraries give gamma-ray production cross sections in the neutron energy range [ $1.10^{-5}$  eV -  $2.10^{+7}$  eV]. Each gamma-ray intensity given in J.K. Tuli's database, initially relative to the thermal neutron energy, is then interpolated to cover the previous energy range.

Thus, NP = 2 for each gamma-ray energy, and NR = 1 corresponds to one interpolation range ending on the second pair of data (NBT = 2), and using a linear interpolation law (INT = 2). LF = 2 means that discrete gamma-rays are described.

LP = 1 means that non-primary photons are created, ES<sub>k</sub> being the energy level from which the photon originate (chosen to be equal to the discrete gamma-ray energy).

For instance, the corresponding first lines of the <sup>76</sup>Ge isotope 12-102 section are presented in Fig. 5.

```

3.207600+4 7.526920+1           1           0           14           0324312102   1
0.000000+0 0.000000+0           0           0           1           2324312102   2
      2           2           0           0           0           0324312102   3
1.000000-5 3.634681-1 2.000000+7 3.634681-1 0.000000+0 0.000000+0324312102   4
5.912850+6 5.912850+6           1           2           1           2324312102   5
      2           2           0           0           0           0324312102   6
1.000000-5 9.266000-2 2.000000+7 9.266000-2 0.000000+0 0.000000+0324312102   7
5.444700+6 5.444700+6           1           2           1           2324312102   8
      2           2           0           0           0           0324312102   9
1.000000-5 4.985100-3 2.000000+7 4.985100-3 0.000000+0 0.000000+0324312102  10
5.420100+6 5.420100+6           1           2           1           2324312102  11
      2           2           0           0           0           0324312102  12
1.000000-5 1.494600-2 2.000000+7 1.494600-2 0.000000+0 0.000000+0324312102  13
    
```

Figure 5. Extract of the <sup>76</sup>Ge isotope 12-102 section.

Fig. 6 gives an example of the 14-102 section added to the 12-102 section below the appropriate separation line (SEND). This section contains ZA, AWR, a parameter indicating whether the photon emission is isotropic (1) or not (0), the number NK of described gamma-rays, and the MAT-MF-MT-N° information. The zeros added in the line just complete this line but have no physical meaning.

```
3.207600+4 7.526920+1      1      0      14      0024314102      1
```

Figure 6. Extract of the  $^{76}\text{Ge}$  isotope 14-102 section.

Finally, the five created isotopic sections are introduced in the ENDF file of the corresponding isotope. The modified ENDF files are then compiled and checked by the NJOY nuclear data processing code [15] to be compatible with the MCNP code (ACE format and corresponding xsdir lines).

#### 4 VALIDATION OF THE NEW GE DATA FILES

The created data files need to be checked and validated before they can be widely used. The validation procedure consists in the following check-list:

- The gamma-ray energies and intensities are checked by comparing simple calculated results with the original database (§ 4.1), and by comparing calculated results to experimental ones using a simplified experimental setup (§ 4.2),
- A comparison is made between calculated and experimental spectra using the complex experimental setup dealt with in § 2.1. Results are presented in paragraph 4.3.

##### 4.1 Simple Calculation Checking

Similarly to the work presented by S.C. Frankle et al. for the photon production data table assessment in MCNP [10], the first step for checking the accuracy of these new data tables is made by comparing a simple flux calculation with J.K. Tuli's data.

The simulation geometry is composed of three concentric spherical volumes. The internal void of 1 cm radius contains a thermal-neutron (0.025 eV) or 14 MeV point source at the centre. The intermediate sphere of 2.5 cm radius is made of natural or isotopic germanium. The Ge density is  $3.52 \text{ g.cm}^{-3}$ . A photon flux (F4 tally) MCNP calculation over the energy range [0-14 MeV] with 1 keV bins is performed in the outer spherical void of 4.5 cm radius.

Fig. 7 shows the calculated result obtained for natural germanium. The germanium gamma-rays appear to be discrete gamma-ray lines, and the comparison between the calculated spectrum and the J.K. Tuli's original data table leads to recognizing all gamma-rays from [2].

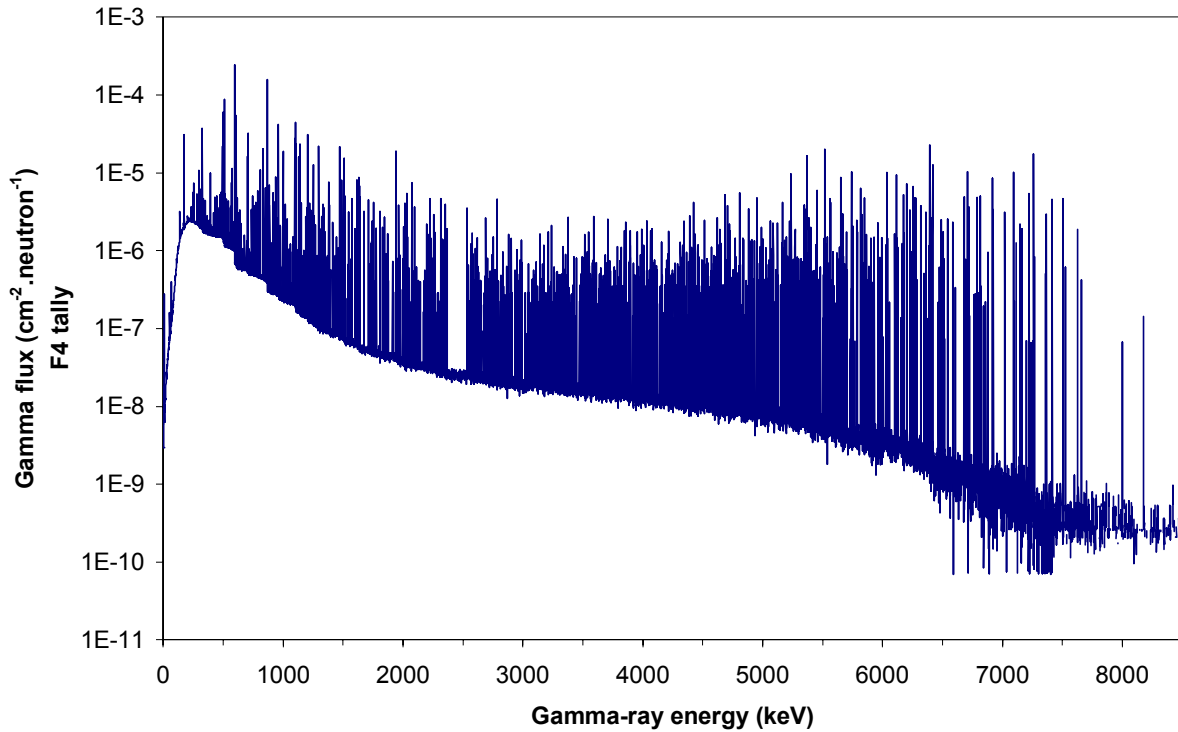


**Figure 7. MCNP calculated signal for natural germanium irradiated with thermal neutrons.**

In order to check the accuracy of the gamma-ray intensities, the net flux (photon.cm<sup>-2</sup>.neutron source<sup>-1</sup>) in each peak of the calculated spectra is determined by subtracting the average background evaluated by interpolating the flux between the two next channels of a given total photo-absorption peak.

The ratio between the two next MCNP net fluxes ( $F=F_i/F_{i+1}$ ) is then compared with the ratio of the corresponding Tuli's intensities ( $I=I_{\gamma_i}/I_{\gamma_{i+1}}$ ) so as to minimize the influence of energy dependent parameters. Fig. 8 shows the variation of the ratio  $I/F$  over the whole gamma-ray energy range for the <sup>73</sup>Ge and <sup>76</sup>Ge isotopes.

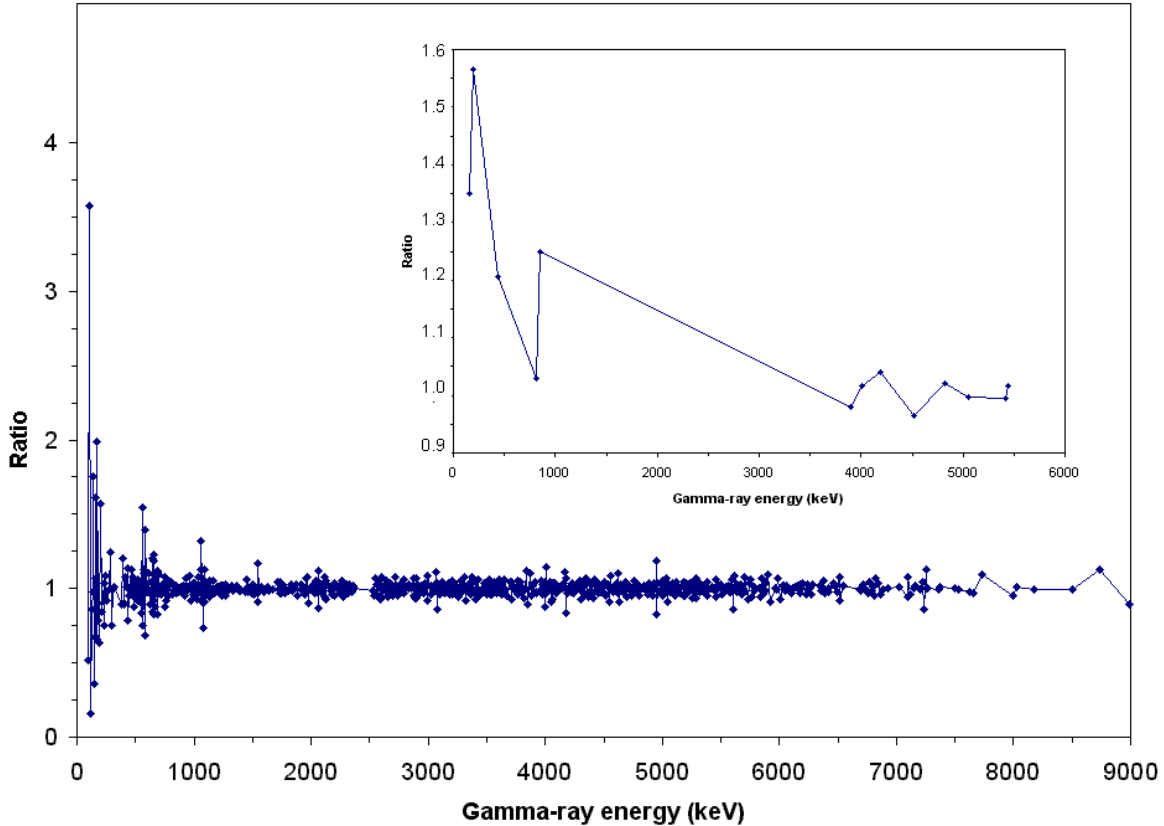


Figure 8. Variation of the calculated ratio I/F with the gamma-ray energies produced by the <sup>73</sup>Ge (principal graph) and <sup>76</sup>Ge (framed graph) isotopes.

The F/I ratio for <sup>73</sup>Ge appears to be close to 1.0. The observed jumps at low energies (below about 500 keV) are due to the variation in the linear attenuation coefficient  $\mu$  at these energies and those at higher energy are linked to the fact that two consecutive peaks may not be so near. The F/I ratio of <sup>76</sup>Ge fluctuates more because of the bigger energy gap between two peaks.

## 4.2 Simple Experimental Checking

This checking point now concerns a comparison between calculated and experimental results.

The basic experimental setup used here is composed of a <sup>252</sup>Cf source ( $10^5 \text{ s}^{-1}$ ) placed at 5.7 cm in front of a GeHP detector in order to induce neutron captures inside the germanium crystal (Fig. 9). The neutrons emitted by the source have a 2 MeV average energy and need to be slowed down to thermal energy in order to increase the neutron capture efficiency in Ge. A polyethylene coffering is used to this end.



**Figure 9. Simplified experimental setup used for the Ge data test.**

The experimental signal shows the presence of Ge, Fe, Ni, Cr, Al and Cu gamma-rays. Many Ge gamma-rays described in Tuli's data table are present on the experimental spectrum. About 18 %<sup>1</sup> of all gamma-rays indicated in [2] appear in the measured signal, while 58 % of the gamma-rays with an intensity greater than 1 % are visible, and 95 % of the gamma-rays with an intensity greater than 5 % can be detected. Considering the whole experimental signal, about 47 % of the observed gamma-rays are due to Ge, including both single and double escapes gamma-rays.

In order to compare experimental to calculated results, MCNP calculations taking into account the new Ge data table created in this way have been performed. The calculated results (direct F8 tally in the Ge detector itself ; a F5 intermediate result is not necessary here) are normalized so as to be compared with the experimental spectrum (Fig. 10).

<sup>1</sup> The <sup>73</sup>Ge isotope produces more than 800 gamma-rays. Only 10 of them have an intensity greater than 5 %, which explains the low percentage of visible gamma-rays

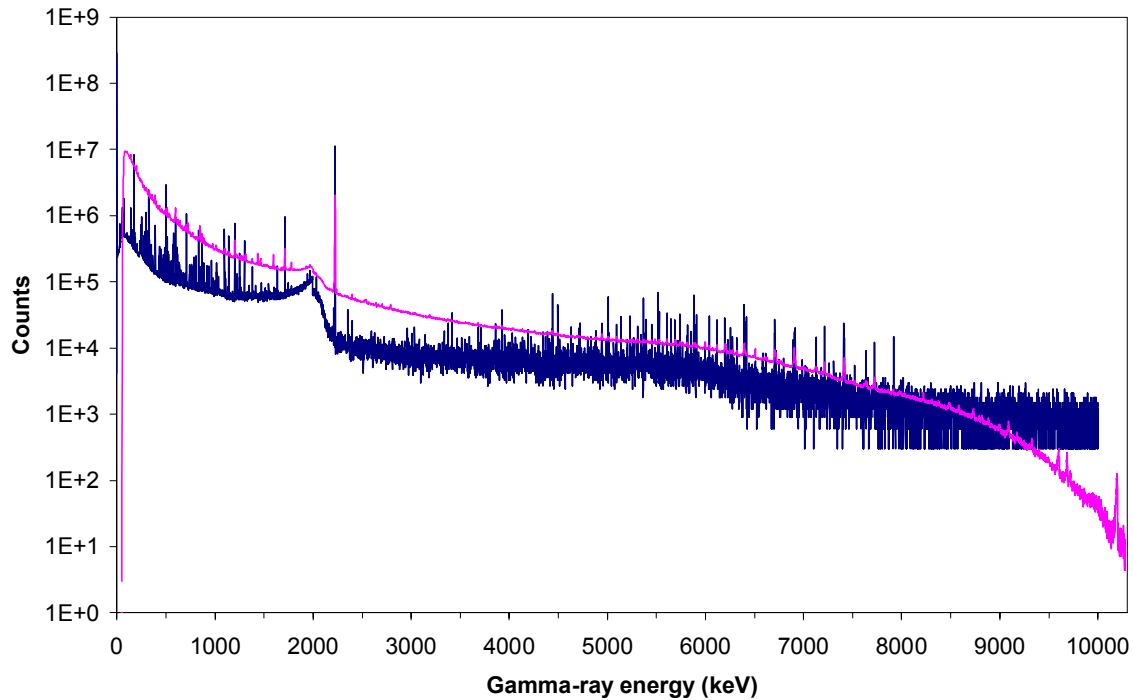


**Figure 10. Comparison between an experimental (pink) and a calculated (blue) spectra obtained with the  $^{252}\text{Cf}$  neutron source.**

The comparison between experimental and calculated spectra shows many similarities concerning the identifiable Ge gamma rays. The isotopic abundance and cross sections [23] of  $^{70}\text{Ge}$  (20.37 % ; 3.43 barns),  $^{72}\text{Ge}$  (27.31 % ; 0.98 barn) and  $^{74}\text{Ge}$  (36.73 % ; 0.51 barn) are such that most of the corresponding gamma-rays appear on both experimental and calculated spectra.

On the other hand, few  $^{73}\text{Ge}$  gamma-rays appear on the spectra in comparison with the great number of gamma-rays tabulated (>800) because of its low natural isotopic abundance (7.76 %) and of the low intensities of most of its gamma-rays. Only the  $^{73}\text{Ge}$  strongest transitions appear at low energy while only some gamma-rays of lower intensities can be seen at higher energy (upon 7 MeV) thanks to the high  $^{73}\text{Ge}$  neutron capture cross section (15 barns).

Finally, only the strongest transition (5912.85 keV, 9.27 %) of the  $^{76}\text{Ge}$  isotope can be seen in the experimental spectrum because  $^{76}\text{Ge}$  has a low isotopic proportion (7.83 %) and a small thermal neutron capture cross section (0.15 barn).

Fig. 11 shows a comparison similar to that in Fig. 10 in the energy range [5000-6000 keV]. The good agreement between the experimental gamma-rays and the calculated ones is here also clearly visible: most of the experimental gamma-rays find their equivalent on the calculated spectrum.

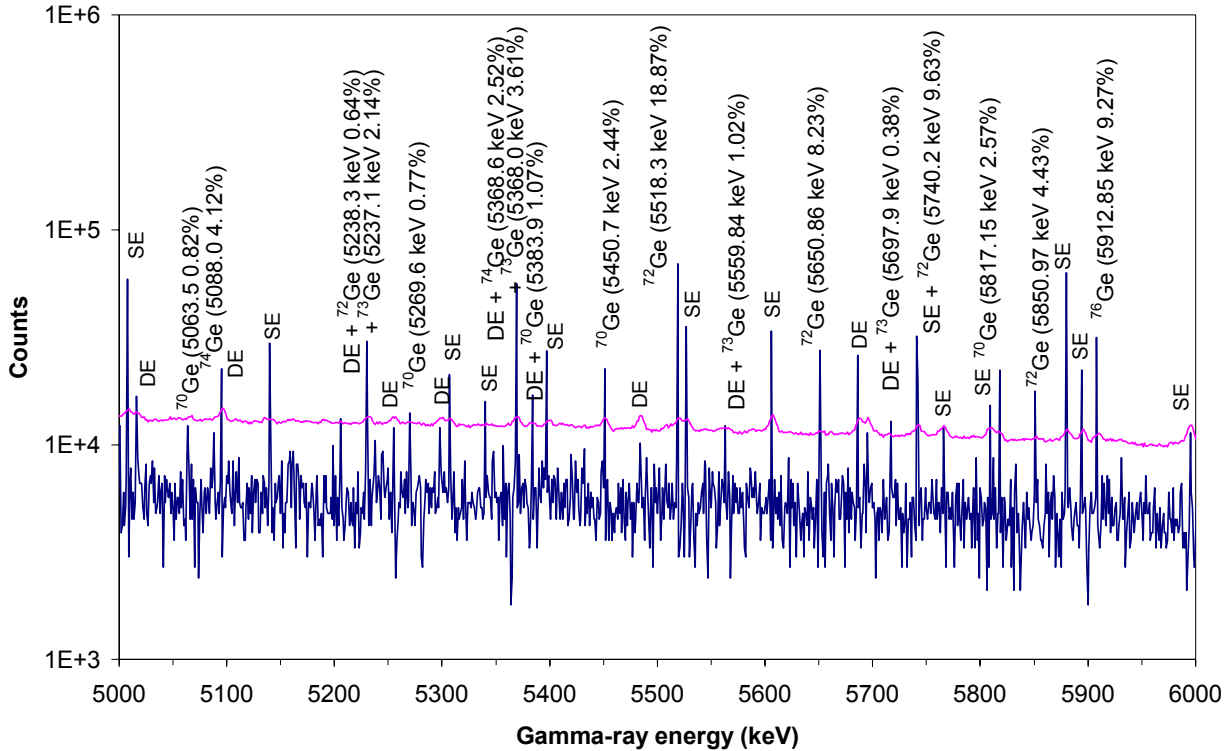


Figure 11. Portion of the calculated (blue) and experimental (pink) spectra obtained with the  $^{252}\text{Cf}$  neutron source.

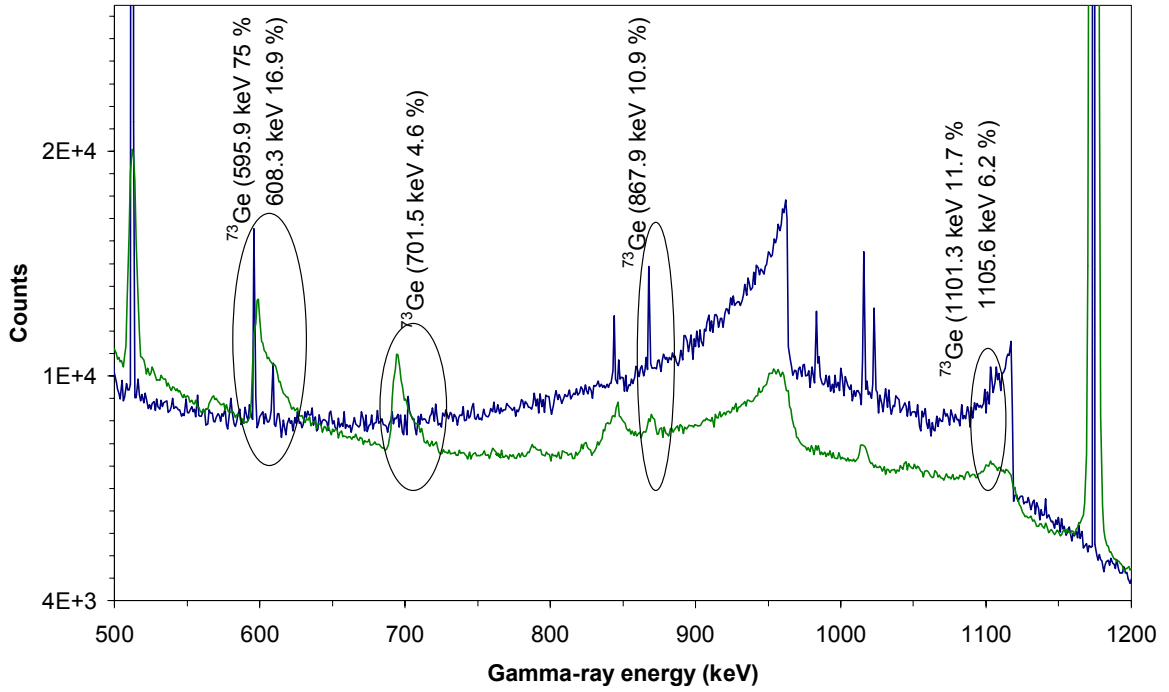
### 4.3 Complex Experimental Data Verification

Fig. 1 shows the comparison between an experimental signal and a preliminary calculated result. Fig. 12 and 13 show a similar comparison in the energy ranges of [500-1200 keV] and [40-190 keV] after the use of ENDF/B-VI release 8 library and the creation of Ge data.

The experimental signal and the calculated result are quite in agreement in the whole energy range, even if not all the Ge gamma-rays introduced in the MCNP data tables appear on the calculated spectrum. However, some of them can be identified and compared to the corresponding gamma-rays appearing in the experimental signal.

Most of the Ge gamma-rays occurring on the calculated spectrum – and thus, in the experimental signal – come from the  $^{73}\text{Ge}$  isotope (Fig. 12). As said before, they correspond to the  $^{73}\text{Ge}$  strongest transitions. Please note that, in that case of complex experimental setup, the  $^{73}\text{Ge}$  gamma-rays are clearly visible whereas, in the former study (§ 4.2), few  $^{73}\text{Ge}$  gamma-rays appeared. This is probably due to the different energy distribution of the incident neutrons between the two configurations, leading to different capture cross sections.

Furthermore, the  $^{72}\text{Ge}$  and  $^{74}\text{Ge}$  identified gamma-rays in the experimental signal do not find their equivalent in the calculated result. (Fig. 13).



**Figure 12.** Comparison between the experimental spectrum (green) and the calculated one with Ge data (blue) in the energy range of [500-1200 keV]. The Ge gamma-rays visible on both spectra are pointed out.

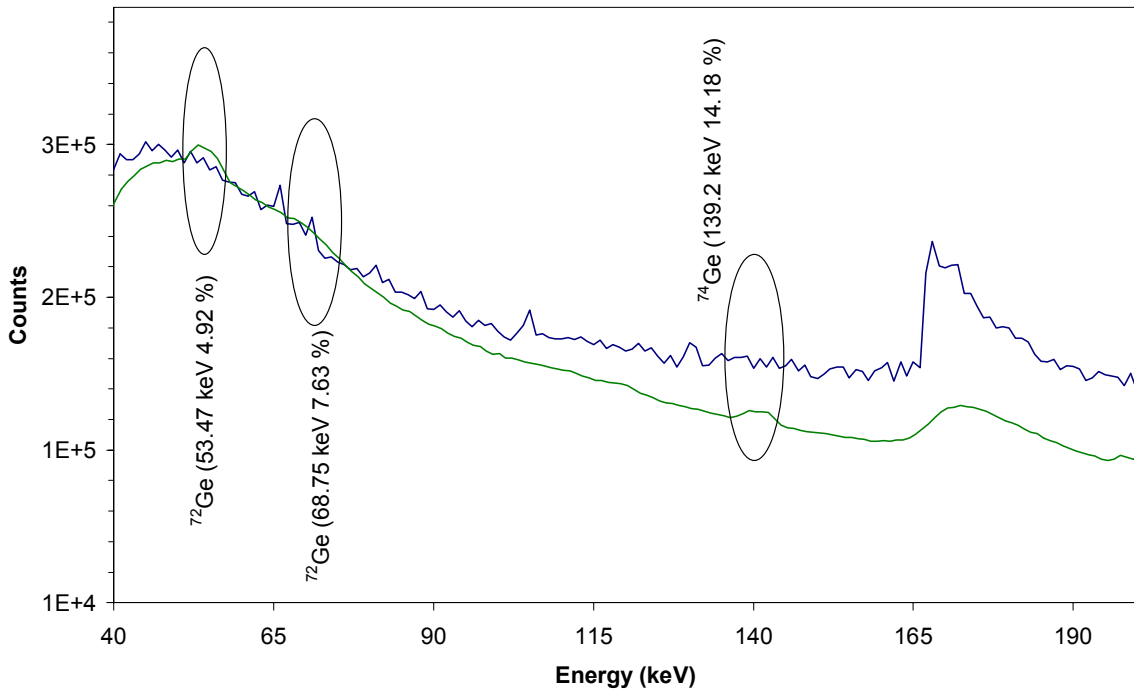


**Figure 13.** Comparison between the experimental spectrum (green) and the calculated one with Ge data (blue) in the energy range of [40-190 keV]. Some Ge gamma-rays invisible on the calculated spectra are pointed out.

## 5 GENERAL CONSIDERATION ABOUT MCNP CALCULATIONS

The difference, observed in § 4.3, between experimental and calculated results may be due to how the calculations are performed (use of a F5 followed by a F8 tallies).

In the case of a complex experimental setup, a direct F8 calculation does not converge in a reasonable time, due to the small dimensions of the detection geometry compared with the large size of the measurement setup.

Furthermore, the chosen F5+F8 calculation way may be quite wrong because the Ge gamma-ray production can not be adequately taken into account. Indeed, Ge gamma-rays are created and detected inside the detector itself, but using an intermediate F5 tally leads first to the count of the Ge gamma-ray contribution in front of the crystal. Gamma-rays are then detected in the crystal itself by using the F8 command and a parallel surface source to the front of the detector.

## 6 CONCLUSIONS

The work presented in this paper mainly concerns the creation of Ge nuclear data tables compatible with the MCNP4C2 calculation code. Based on data published by J.K. Tuli [2] formerly lacking 12-102 and 14-102 sections [8] have been created. They were added to the existing cross-sections Ge files in Jeff3.0 library and compiled.

The data were then successfully checked by various comparisons including a comparison between the original data and calculated results, and comparisons between experimental and calculated results using a simple and a complex experimental setup. Gamma-rays energies could then be identified from both experimental and calculated results.

The validation of gamma-rays intensities is more difficult to finalize, as it depends on the comparison of experimental and calculated total photo-absorption peaks areas, including other independent parameters that can be difficult to evaluate.

## 7 ACKNOWLEDGMENTS

We wish to thank our colleagues Mrs. A. Lamarche and M. J-L. Ma for their contribution to the calculation and experimental work, respectively, and M. J-C. Sublet for his help in the nuclear data research and processing approach.

## 8 REFERENCES

[1] J.F. Briesmeister Ed., "MCNP Monte-Carlo N-Particle transport code, Version 4C" . Los Alamos National Laboratory report LA-13709-M (2000).

[2] J.K. Tuli, "Thermal neutron capture gamma-rays," <http://www.nndc.bnl.gov/capgam/>

[3] P. Pin, B. Perot, "Self-induced X-ray Fluorescence and Peak/Compton Comparison: Two Innovative Methods for Bituminized Waste Drum Characterization," *International Youth Nuclear Congress*, Toronto, Canada (2004).

[4] C. Passard, A. Mariani, F. Jallu, J. Romeyer-Dherbey, H. Recroix, M. Rodriguez, J. Loridon, C. Denis, H. Toubon, "PROMETHEE: An Alpha Low-level Waste Assay System using Passive and Active Neutron Measurement Methods," *Nuclear Technology*, **140**, pp.303-314 (Dec. 2002).

[5] R. Thierry, J-L. Pettier, L. Desbat, "Simultaneous Compensation for Attenuation Scatter and Detector Response for two Dimensional Emission Tomography on Nuclear Waste Reduced Data," *Proceedings of the First World Congress on Industrial Process Tomography*, Buxton, UK, p.542 (Apr. 1999).

[6] J-L. Ma, A. Mariani, C. Passard, M. Rodriguez, "PGNAA applied to direct Measurement of  $^{129}\text{I}$  - Preliminary Works," *Proceedings of the 9th Symposium on Capture Gamma-ray Spectroscopy and Related Topics*, Budapest, Hungary, 8-12 Oct. 1996, Vol.2, p.721-725.

[7] J.S. Hendricks, S.C. Frankle, J.D. Court, "ENDF/B-VI Data for MCNP," Los Alamos National Laboratory report LA-12891 (1994).

[8] "ENDF-102 Data Format and Procedure for the Evaluated Nuclear Data File ENDF-6," V. Mc Lane Ed. , BNL-NCS-44954-01/04 Rev., <http://www.nndc.bnl.gov/nndcscr/documents/endl/endl102/> (April 2001).

[9] S.C. Frankle, "Criticality Benchmark Results using various MCNP Data Libraries," Los Alamos National Laboratory report LA-13627 (July 1999).

[10] S.C. Frankle, "Photon Production Assessment for the MCNP Data Libraries," Los Alamos National Laboratory report LA-13092-MS, <http://www-xdiv.lanl.gov/PROJECTS/DATA/nuclear/pdf/LA-13092-MS.pdf> (Mar. 1996).

[11] "Photon production in the MCNP data libraries, DISCEGAM ", <http://www-xdiv.lanl.gov/PROJECTS/DATA/nuclear/photon/photon.html> (last revision December 2003).

[12] J.M. Campbell, S.C. Frankle, R.C. Little, "ENDF66: A Continuous-energy Neutron Data Library for MCNP4C," *Proceedings of the 12<sup>th</sup> Biennial Radiation Protection and Shielding Topical Meeting*, Santa Fe, New-Mexico, USA, 15-19 April 2002.

[13] S.C. Frankle, R.C. Reedy, P.G. Young, "ACTI: An MCNP Data Library for Prompt Gamma-ray Spectroscopy," *Proceedings of the 12<sup>th</sup> Biennial Radiation Protection and Shielding Topical Meeting*, Santa Fe, New-Mexico, USA, 15-19 April 2002.

[14] J.C. Sublet, Private Communication.

[15] "The NJOY Nuclear Data Processing System," <http://www.t2.lanl.gov/njoy/>

[16] "The Jeff-3.0 Nuclear Data Library", [http://www.nea.fr/html/dbdata/projects/nds\\_jef.htm](http://www.nea.fr/html/dbdata/projects/nds_jef.htm)

[17] M.A. Lone, R.A. Leavitt, D.A. Harisson, "Prompt Gamma Rays from Thermal Neutron Capture," *Atomic Data and Nuclear Data Tables*, **26**, p.511 (1981).

[18] S.C. Frankle, R.C. Reedy, P.G. Young, "Improved Photon Production Data for Thermal Neutron Capture in the ENDF/B-VI Evaluations," Los Alamos National Laboratory report LA 13812, <http://www-xdiv.lanl.gov/PROJECTS/DATA/nuclear/photon/ge.htm> (Jun. 2001).

[19] "EXFOR, Experimental nuclear reaction data retrieval" <http://www.nea.fr/html/dbdata/x4/welcome.html>

[20] E. Weishaupt, D. Rabenstein, "Contribution to the Level Schemes of Ge-71, Ge-73, Ge-74 and Ge-75 from a Study of the (n,  $\gamma$ ) Reactions in Natural Germanium," *Zeitschrift für Physik*, **251**, p. 105 (Jun. 1972) EXFOR Ref. 20966.002.

[21] A. Hasselgren, "Deuteron Stripping and Thermal Neutron Capture Gamma Reactions on the Ge-72, -74 and -76 Isotopes," *Nuclear Physics*, **A198**, p.353 (1972), EXFOR Ref. 20227.002, 20227.003, 20227.004, 20227.005, 20227.006.

[22] A.P. Magruder, R.K.Smith, "<sup>73</sup>Ge(n,  $\gamma$ )<sup>74</sup>Ge Gamma-Ray Spectrum and Energy Levels," *Physical Review*, **183**, p. 927 (Jul. 1979) EXFOR Ref. 13821.002.

[23] M. Antony, "Nuclide Chart 2002," Strasbourg, France (2002)